HOKKAIDO UNIVERSITY

Title	Spatial variations in larch needle and soil 15N at a forest–grassland boundary in northern Mongolia
Author(s)	Fujiyoshi, Lei; Sugimoto, Atsuko; Tsukuura, Akemi; Kitayama, Asami; Lopez Caceres, M. Larry; Mijidsuren, Byambasuren; Saraadanbazar, Ariunaa; Tsujimura, Maki
Citation	Isotopes in Environmental and Health Studies, 53(1), 54-69 https://doi.org/10.1080/10256016.2016.1206093
Issue Date	2016
Doc URL	http://hdl.handle.net/2115/73948
Rights	This is an Accepted Manuscript of an article published by Taylor & Francis in ISOTOPES IN ENVIRONMENTAL AND HEALTH STUDIES on 2017, available online: http://www.tandfonline.com/doi/full/10.1080/10256016.2016.1206093
Type	article (author version)
File Information	Fujiyoshi2017_HUSCAP.pdf

Instructions for use

1 **Spatial variations in larch needle and soil $\delta^{15}N$ at a forest-grassland**

2 **boundary in northern Mongolia**

3 Lei Fujiyoshi[1], Atsuko Sugimoto[1, 2, 3*], Akemi Tsukuura[1], Asami Kitayama[1],

4 M. Larry Lopez Caceres[4], Byambasuren Mijidsuren[5], Ariunaa Saraadanzar[5],

5 Maki Tsujimura[6]

6 *[1]Graduate School of Environmental Science, Hokkaido University, Sapporo, Hokkaido*

7 *060-0810, Japan*

8 *Phone: +81-(0)11-706-2233*

9 *[2]Faculty of Environmental Earth Science, Hokkaido University, Sapporo, Hokkaido*

10 *060-0810, Japan*

11 *Phone: +81-(0)11-706-2233*

12 *[3]Arctic Research Center, Hokkaido University, Sapporo, Hokkaido 001-0021, Japan*

13 *Phone: +81-(0)11-706-9075*

14 *[4]Faculty of Agriculture, Yamagata University, Tsuruoka, Yamagata 997-8555, Japan*

15 *Phone: +81-(0)23-528-2805*

16 *[5]Plant Protection Research Institute, Mongolian University of Life Sciences, Zaisan*

17 *210153, Ulaanbaatar, Mongolia*

18 *Phone: +976-11-345212*

19 *6Faculty of Life and Environmental Sciences, University of Tsukuba, Tsukuba, Ibaraki*

20 *305-8572, Japan*

21 *Phone: +81-(0)29-853-2568*

22 e-mail:

23 Lei Fujiyoshi (green-nandin@ees.hokucai.ac.jp), *Atsuko Sugimoto

24 (sugimoto@star.dti2.ne.jp), Akemi Tsukuura (akemi.tsukuura@gmail.com), Asami

25 Kitayama (asami.kitayama@ees.hokudai.ac.jp), M. Larry Lopez Caceres

26 (larry@tds1.tr.yamagata-u.ac.jp), Byambasuren Mijidsuren (byamba0730@yahoo.com),

27 Ariunaa Saraadanzar (ardiu99@yahoo.com), Maki Tsujimura

28 (mktsuji@geoenv.tsukuba.ac.jp)

29 *Correspondence to: Atsuko Sugimoto   (sugimoto@star.dti2.ne.jp)

30

34

35

36

Spatial variations in larch needle and soil δ^{15}N at a forest-grassland boundary in northern Mongolia

The spatial patterns of plant and soil δ^{15}N and associated processes in the N cycle were investigated at a forest-grassland boundary in northern Mongolia. Needles of *Larix sibirica* Ledeb. and soils collected from two study areas were analysed to calculate the differences in δ^{15}N between needle and soil ($\Delta\delta^{15}$N). $\Delta\delta^{15}$N showed a clear variation, ranging from -8‰ in the forest to -2‰ in the grassland boundary, and corresponded to the accumulation of organic layer. In the forest, the separation of available N produced in the soil with ^{15}N-depleted N uptake by larch and ^{15}N-enriched N immobilization by microorganisms was proposed to cause large $\Delta\delta^{15}$N, whereas in the grassland boundary, small $\Delta\delta^{15}$N was explained by the transport of the most available N into larch. The divergence of available N between larch and microorganisms in the soil, and the accumulation of diverged N in the organic layer control the variation in $\Delta\delta^{15}$N.

54

1. Introduction

Nitrogen (N) is one of the key elements in biological processes. The N cycle in

plant-soil system includes the decomposition of soil organic matter, the uptake of

biologically available N (e.g. NH_4^+ and NO_3^-) by plants and soil microorganisms, and

the return of litterfall to the soil as an internal processes, as well the N input as

atmospheric deposition and/or biological N_2 fixation, and the loss by leaching and/or

gaseous emission as external processes [1]. All these processes result in variations in

plant and soil $\delta^{15}N$, which are caused by differences in the $\delta^{15}N$ of sources for plants [2],

N loss, such as nitrate (NO_3^-) leaching [3] or gaseous emission (N_2O, N_2) via

nitrification and denitrification [4], decomposition processes, such as mineralization and

nitrification[5], mycorrhizal fungi [6], and physiological processes within the plant [7].

As a result, plant and soil $\delta^{15}N$ serve as useful indicators of the N cycle in the plant-soil

system [8].

The $\delta^{15}N$ values of plant and soil in forest ecosystem have been investigated and

various characteristics have been reported [9]. The plant $\delta^{15}N$ values of co-occurring

species in boreal forest showed differences among species, which were attributed to the

different N source for each species in terms of N form and/or the depth of N uptake [10].

72 On the other hand, it has been shown that soil $\delta^{15}N$ generally increases with depth, from

73 organic layer which is typically observed in forest, to mineral soil [11]. Previous studies

74 also showed that the organic layer contributes as significant nitrogen source for trees

75 [12, 13]. Furthermore, recent global syntheses in $\delta^{15}N$ values have shown the spatial

76 trends in $\delta^{15}N$ values of plant and soil along climate gradient [14–16].

77 　　The difference between plant and soil $\delta^{15}N$ ($\Delta\delta^{15}N$ = plant $\delta^{15}N$ - soil $\delta^{15}N$), which is

78 an apparent enrichment factor, allows the comparison of different sites by normalizing

79 the spatial heterogeneity in soil $\delta^{15}N$ [17].$\Delta\delta^{15}N$ has been widely applied, and variations

80 in $\Delta\delta^{15}N$ have been attributed to various causes such as differences in N forms that plant

81 uptake (DON, NH_4^+, or NO_3^-) [17–22] and changes in $\delta^{15}N$ of each N form affected by

82 nitrification [17,18,23,24]. Mycorrhizal fungi have also been reported to affect $\delta^{15}N$

83 through ^{15}N-enrichment in the fungal body [25], although the degree of enrichment is

84 still controversial [26]. Not only these internal processes within the plant-soil system,

85 but also atmospheric N deposition that serve as the N source for plants [27], has been

86 reported to cause variations in $\Delta\delta^{15}N$. Additionally, the strategy of field observations

87 often complicates the interpretation of $\Delta\delta^{15}N$. Previous studies set wide spatial scales

88 (region, country, or globe) along the gradient of specific environmental variables

89 (climate, topography, soil age, and parent material), which hampered the interpretation

90   of $\Delta\delta^{15}N$, due to the needed comparison among different plant species with different

91   degrees of isotopic fractionation within the plant body [7], and the co-existence of

92   variables that affect plant and soil $\delta^{15}N$ [14].

93   In this study, we investigated a forest-grassland boundary (ecotone) ecosystem in

94   northern Mongolia, in which vegetation changes from Siberian larch (*Larix sibirica*

95   Ledeb.) forest to temperate grassland within a very short distance of a few kilometres.

96   Investigation of this ecotone offered the following advantages: (1) existence of a single

97   plant species (*L. sibirica* Ledeb.) that allowed comparisons along the forest-grassland

98   gradient, and (2) exclusion of variables such as climate, soil age, and parent material

99   which were considered similar at all sites within this region. Therefore, this study aimed

100 to clarify the spatial patterns and underlying mechanisms that control $\Delta\delta^{15}N$ which arise

101 only from the differences between forest and grassland ecosystems.

102

103

104 **2.   Materials and methods**

105 **2.1.   *Site description***

106 Two study areas, Terelj (TR) and Mongonmorit (MM), were chosen for sampling at a

107 forest-grassland boundary in northern Mongolia (Figure 1(a)). Information on site

108   locations and positions is presented in Table 1. The forest consists of Siberian larch

109   (*Larix sibirica* Ledeb.) and white birch (*Betula platyphylla* Sukach.) in some places

110   [28,29]. This region corresponds to the southern boundary of permafrost [29], which

111   coincides with the distribution of boreal forest. The forest dominates the north-facing

112   slopes, whereas temperate grassland dominates the south-facing slopes, dry valleys, and

113   flat plains [29]. The soil in this region is cryosol, and the climate is cold continental

114   climate with dry winters, according to Köppen-Geiger climate classification [30]. The

115   mean annual temperature (MAT) is -3.6°C in TR area and -2.9°C in MM area, and

116   average temperature from May to September is 10.4°C in TR area and 11.2°C in MM

117   area. The mean annual precipitation (MAP) is 353 mm in TR area and 272 mm in MM

118   area, whereas 90% of precipitation occurs during the growing season of larch trees

119   (May to September) [28].

120   In this study, samplings were conducted along the forest-grassland gradient, and the

121   sampling sites were classified as forest or boundary as described by Tuhkanen [31].

122   Forest site was defined as the site in the continuous forest, whereas boundary site was

123   defined as the site between the edge of continuous forest and grassland. In TR area,

124   sampling was conducted along a transect from the north-facing slope to the south-facing

125   slope over a valley at 11 sites (TR1n to TR2s) (Figure 1(b)), whereas in MM area, two

126 transects were set on the south-facing slope and southwest-facing slope and sampling

127 was conducted at 10 sites (MM1sw to MM7s) (Figure 1(c)). Among the 21 sites in total,

128 6 sites in TR area (TR1n to TR6n) and 6 sites in MM area (MM1sw to MM3s) were

129 forest sites, and the rest were boundary sites, except for patchy forest (TR1s) and

130 grassland site with no trees (TR2s) in TR area. Both TR and MM areas included

131 forest-grassland gradient, however MM area had more boundary sites with sparser tree

132 distribution on south-facing slope. Observations at those sites in these two areas covered

133 all range of forest-grassland gradient, and also wide range of conditions regarding

134 organic layer accumulation (litter, fermentation, and humus), which was relatively rich

135 in forest sites (mor-type) to poor in boundary sites (mull-type) [32].

136 [Figure 1 and Table 1 near here]

137

138 **2.2. *Sampling***

139 2.2.1. *Foliar samples*

140 Larch needles were collected during the growing season (May to August) from 2004 to

141 2012. Needles from three to four branches at a height of 1 to 5 m were taken from each

142 tree. More than three trees were usually sampled at each site, but only one or two trees

143 in boundary sites due to their limited number. Needles were also collected from several

144 trees at three sites in TR area (TR3n, TR6n, and TR1s) and two sites in MM area

145 (MM2s and MM1sw) during the growing season of 2004 and 2005 to evaluate temporal

146 variations. Needle samples were oven-dried at 60°C, milled, and wrapped in tin cups for

147 analysis.

148 2.2.2. *Soil samples*

149 Soil samples were collected at the same sites as needle samples. A small pit (0.6 m × 0.6

150 m × 0.6 m deep) was made, and one to three cores (1.5 cm diameter, 4.5 cm length) of

151 bulk soil were collected from the cross section of the pit every 10 cm from 0 cm (the top

152 of mineral soil) down to 50 cm depth or until a rock appeared. The organic layer was

153 also sampled by collecting the organic matter above the mineral soil. The fresh soil

154 samples were sieved with a 2 mm mesh to remove gravel and living roots, oven-dried at

155 105°C for more than 24 h, and used for isotope analysis. Fresh soil samples collected in

156 2012 were also used for KCl-extractable N (DON, NH_4^+, and NO_3^-) analysis.

157

158 **2.3. *Analysis***

159 2.3.1. *C/ N isotopic ratio and concentrations*

160 The $\delta^{13}C$, $\delta^{15}N$, and C, N concentrations were analysed using Conflo system with

161 DELTA V Plus and FlashEA 1112 (Thermo Fisher Scientific) at the Graduate School of

162   Environmental Science, Hokkaido University, Japan. The isotope ratio was expressed

163   using the δ notation:

164    $\delta^{15}N$ (or $\delta^{13}C$) = $\left(\dfrac{R_{sample}}{R_{std}} - 1 \right) \times 1000$ (‰)

165   where R_{sample} is the isotope ratio ($^{13}C/^{12}C$ or $^{15}N/^{14}N$) of a sample, and R_{std} is the isotope

166   ratio ($^{13}C/^{12}C$ or $^{15}N/^{14}N$) of Vienna Pee Dee Belemnite (VPDB) or atmospheric N_2 for

167   C and N. Analytical errors were at 0.2‰ for $\delta^{13}C$, 0.3‰ for $\delta^{15}N$, 0.5% for the bulk C

168   concentration, and 0.1% for the bulk N concentration.

169   2.3.2.   *KCl-extractable N*

170   Soil N pools (DON, NH_4^+, and NO_3^-) were extracted from 4 g of fresh soil with 40 ml of

171   2M KCl after 1 h of shaking and filtration. The extracts were kept in coolers,

172   transported to the laboratory, and stored in a freezer until analysis. The concentration of

173   NO_3^-, NH_4^+, and total dissolved N (TDN) was analysed colorimetrically using a

174   continuous flow nutrient analyser (QuAAtro; BRAN+LUEBBE, Hamburg, Germany).

175   Then, the concentration of dissolved organic N (DON) was calculated by subtracting

176   total inorganic N (NO_3^- and NH_4^+) from TDN. The concentration of nitrite (NO_2^-) was

177   also analysed, but not detected in any samples.

178   2.3.3.   *Calculation of average values at each site*

179   To obtain needle N concentration, $\delta^{15}N$, and $\delta^{13}C$ at each site, data were first averaged

10

180   for all trees in each sampling period excluding those obtained in May, and then

181   averaged for all sampling periods at each site. Needle $\delta^{15}N$, $\delta^{13}C$, and N concentrations

182   observed on all sampling dates at each site are shown in Figure S1. For bulk soil $\delta^{15}N$ at

183   each site, the weighted mean of $\delta^{15}N$ in the 0-20 cm soil layer was calculated from all

184   the available data. The mean N concentration and the C/N ratio in the 0-20 cm soil layer

185   at each site were also calculated from all the available data. $\Delta\delta^{15}N$ was calculated as

186   (needle $\delta^{15}N$ – soil $\delta^{15}N$) at each site.

187   2.3.4.   *Isotope mass balance on available N*

188   To interpret the processes reflected in the variation of $\Delta\delta^{15}N$, we applied the mass

189   balance of biologically available N. Assuming that the available N pool is at a steady

190   state, the following equations are established:

191    $$F_{input} + F_a = F_p + F_m + F_{leach} + F_{gas} \tag{1}$$

192   and for $\delta^{15}N$,

193    $$F_{input} \times \delta_{input} + F_a \times \delta_a = F_p \times \delta_p + F_m \times \delta_m + F_{leach} \times \delta_{leach} + F_{gas} \times \delta_{gas} \tag{2}$$

194   where F_{input} is the N derived from atmospheric N deposition and biological N_2 fixation,

195   and F_a is the N produced in the soil through the decomposition of soil organic matter. F_P

196   and F_m are the fluxes of available N taken up by plants and immobilized by soil

197   microorganisms, respectively. F_{leach} and F_{gas} are the N lost due to leaching and gaseous

198   emission, respectively. The values of δ_{input}, δ_a, δ_p, δ_m, δ_{leach}, and δ_{gas} are the $\delta^{15}N$ of input,

199   produced N from soil organic matter, plant uptake, immobilization by soil

200   microorganisms, leaching, and gaseous emission of available N, respectively. We

201   assumed that larch was the only plant species (i.e. δ_p = needle $\delta^{15}N$), and that the $\delta^{15}N$ of

202   available N produced in the soil was the same as that of the soil (i.e. δ_a = soil $\delta^{15}N$).

203   Generally, available N produced in the soil has similar $\delta^{15}N$ to that of soil organic matter,

204   if all produced N remains in the N pool without any fractionated loss [33]. The

205   schematic representation of each process is shown in Figure S2.

206   2.3.5.   *Statistical analysis*

207   The temporal variation of tree components was evaluated by Wilcoxon signed-rank test

208   at $p < 0.05$ (two-tailed). The spatial relationships between the variables were evaluated

209   by Spearman's rank correlation coefficient at $p < 0.05$ (two-tailed).

210

211

212   **3.   Results**

213   **3.1.   *Temporal variations in $\delta^{15}N$, $\delta^{13}C$, and N concentration of larch needles***

214   Temporal variations in needle N concentration, $\delta^{15}N$, and $\delta^{13}C$ of nine individual trees

215   were observed during the growing season of 2004 and in July 2005 at three sites in TR

216   area (TR3n, TR6n, and TR1s) (Figure 2). Needle N concentrations were significantly

217   higher in May 2004 than the following months in 2004 and July in 2005 ($p < 0.05$)

218   (Figure 2(a)). Temporal changes or inter-annual variations were not observed for $\delta^{15}N$

219   and $\delta^{13}C$ (Figure 2(b) and 2(c)). The same temporal variations were also observed in

220   MM area (data not shown). When the data collected in May were excluded, the standard

221   deviations of individual trees during the observed period were 0.4%, 0.5‰, and 0.9‰

222   for N concentration, $\delta^{15}N$, and $\delta^{13}C$, respectively.

223   [Figure 2 near here]

224

225   **3.2.   *Vertical profile of larch needle, organic layer, and bulk soil $\delta^{15}N$***

226   The $\delta^{15}N$ value increased vertically from needle, organic layer to soil with depth, and

227   also differed between forest and boundary sites, as seen in the example for TR area

228   (Figure 3). At the forest site (TR1n) and the boundary site (TR7n), soil $\delta^{15}N$ increased

229   up to 20-30 cm soil depth. This pattern in soil $\delta^{15}N$ was common at all sites in TR and

230   MM areas. However, changes in the $\delta^{15}N$ of needle, organic layer, and soil were

231   different between the two sites; a gradual increase in $\delta^{15}N$ was observed at TR1n,

232   whereas a slight increase was observed at TR7n. Similarly, in MM area, a gradual

233   increase in the $\delta^{15}N$ from needle, organic layer to soil was observed at the forest site

13

234   (MM2sw), whereas slight increase was observed at the boundary sites, especially at

235   MM5s, MM6s and MM7s (data not shown). [Figure 3 near here]

236

237   **3.3.   *Spatial variations along the forest-grassland gradient***

238   Characteristic spatial patterns in $\delta^{15}N$ values, needle $\delta^{13}C$, and needle N concentration

239   were observed along the forest-grassland gradient in TR and MM areas (Figure 4). In

240   TR area, needle $\delta^{15}N$ increased gradually from -3.9‰ at the forest site (TR1n) to +3.3‰

241   at the boundary site (TR8n) on the north-facing slope, whereas on the south-facing

242   slope, needle $\delta^{15}N$ at TR1s in the patch forest (+1.2‰) was similar to that at TR6n and

243   slightly lower than that at TR8n. In contrast to needle $\delta^{15}N$, soil $\delta^{15}N$ slightly varied

244   from +2.9‰ at TR2n to +5.3‰ at TR7n on the north-facing slope, whereas it was

245   higher on the south-facing slope at TR1s (+5.8‰) and TR2s (+7.4‰). The values of

246   $\Delta\delta^{15}N$ showed the same pattern as needle $\delta^{15}N$ on the north-facing slope (Figure 4(b));

247   $\Delta\delta^{15}N$ was larger in the forest (-8‰ at TR1n) and smaller in the boundary (-3‰ at

248   TR7n) on the north-facing slope, whereas $\Delta\delta^{15}N$ at TR1s on the south-facing slope

249   (-5‰) was similar to that at TR5n. On the north-facing slope, needle $\delta^{13}C$ increased

250   from -27.8‰ to -26.2‰ from the forest site (TR1n) to the boundary site (TR8n), and

251   needle N concentration also increased from 2.0% to 2.7%, respectively. On the

252 south-facing slope, needle $\delta^{13}C$ at TR1s (-26.0‰) was as high as that at TR8n, and

253 needle N concentration at TR1s (2.4%) was similar to that at TR7n (Figure 4(c)).

254 KCl-extractable N (DON, NH_4^+, and NO_3^-) pools in the 0-20 cm soil layer were

255 observed at two forest sites on the north-facing slope (TR2n and TR5n) in August 2012

256 (Table S1). At both sites, DON was more than one-order of magnitude larger than NH_4^+

257 and NO_3^- pools. Additionally, NH_4^+ pool was larger than NO_3^- pool with lower NO_3^- to

258 NH_4^+ ratios (< 0.2).

259   In MM area, needle $\delta^{15}N$ values were higher on the south-facing slope (+2.7‰ to

260 +4.3‰) where most sites were located in the boundary, than those on the

261 southwest-facing slope (+0.34‰ to +2.0‰) where all sites were located in the forest

262 (Figure 4(d)). In contrast, soil $\delta^{15}N$ slightly varied (+5.1 to +6.8‰) in MM area. The

263 $\Delta\delta^{15}N$ slightly changed from -4‰ to -2‰ at the sites on the south-facing slope, which

264 were smaller than those on the southwest-facing slope (-6‰) (Figure 4(e)). Needle $\delta^{13}C$

265 and needle N concentration were higher at the sites on the south-facing slope (-26.2‰

266 to -24.6‰) than those on the southwest-facing slope (-27.5‰ to -26.2‰) (Figure 4(f)).

267 KCl-extractable N (DON, NH_4^+, and NO_3^-) pools in the 0-20 cm soil layer were

268 observed at one forest site (MM3s) and three boundary sites (MM4s, MM5s, and

269 MM6s) on the south-facing slope in August 2012 (Table S1). The DON pool was more

270 than one-order of magnitude larger than NH_4^+ and NO_3^- pools at all sites, just as

271 observed in TR area. However, unlike forest sites in TR area, NO_3^- pool size was

272 similar to that of NH_4^+ at boundary sites (MM4s, MM5s, and MM6s), namely high NO_3^-

273 to NH_4^+ ratios (close to 1).

274 [Figure 4 near here]

275

276 **3.4.** *Relationships between $\delta^{15}N$ values and other parameters*

277 Significant correlations between different variables of all the sites in TR and MM areas

278 were observed (Figure 5). The correlation was observed between needle $\delta^{13}C$ and needle

279 $\delta^{15}N$ ($r_s = 0.877$) (Figure 5(a)), soil $\delta^{15}N$ and needle $\delta^{15}N$ ($r_s = 0.718$) (Figure 5(b)),

280 needle N concentration and $\Delta\delta^{15}N$ ($r_s = 0.591$) (Figure 5(c)), and C/N ratio of bulk soil

281 and $\Delta\delta^{15}N$ ($r_s = -0.541$) (Figure 5(d)). Data in MM area showed small $\Delta\delta^{15}N$ (-5‰ to

282 -2‰), high needle $\delta^{15}N$ (+0.34‰ to +4.3‰), high soil $\delta^{15}N$ (+5.1‰ to +6.8‰), whereas

283 in TR area showed larger variations in those values.

284 [Figure 5 near here]

285

286

287 **4. Discussion**

288 In this study, we observed large spatial variations in needle $\delta^{15}N$ and the difference

289 between needle and soil $\delta^{15}N$ ($\Delta\delta^{15}N$) at each area, whereas relatively small variation in

290 soil $\delta^{15}N$ (Figure 5(b)). The range of $\Delta\delta^{15}N$ observed in this study (6‰) (Figure 5(b))

291 accounts for a half of the global latitudinal variation [14], despite the same plant species

292 (*L. sibirica* Ledeb.), soil age, land use history, and climate. The spatial variation in

293 $\Delta\delta^{15}N$ indicates that the N cycle changes along the forest-grassland gradient. Here, the

294 isotope mass balance of available N in the soil was applied to understand the

295 mechanism of variation in $\Delta\delta^{15}N$.

296   First, we simplify the mass balance equations by deleting some terms in the equations

297 (1) and (2). Assuming a steady state condition of plant and soil N pools in the system,

298 the flux of input equals to that of loss ($F_{input} = F_{leach} + F_{gas}$), and then the equations (1)

299 and (2) can be simplified as follows:

300 $$F_a = F_p + F_m \tag{3}$$

301 $$\delta_a = \delta_s = f \times \delta_p + (1-f) \times \delta_m \tag{4}$$

302 where δ_s is soil $\delta^{15}N$, and f is the fraction of available N which is transported to the

303 plants ($f = F_p/F_a$). Namely, under a steady state condition, available N produced in the

304 soil is transported to plants and microorganisms. We assume that larch is the only plant

305 species (i.e. δ_p = needle $\delta^{15}N$), and also $\delta^{15}N$ of available N produced in the soil is the

306 same as that of the soil (i.e. $\delta_a = \delta_s$) as described in the Materials and methods. We focus

307 on the 0-20 cm soil layer to apply this mass balance, since all sites showed significant

308 increase in soil $\delta^{15}N$ at this layer (Figure 3), in which an active decomposition of soil

309 organic matter occurs [33].

310   From these equations, two processes could explain the small difference in $\delta^{15}N$

311 between larch needle and soil ($\Delta\delta^{15}N \cong 0$) observed at boundary sites (Figure 5(b)): (1)

312 available N is transported to larch and/or microorganisms without significant

313 fractionation ($\delta_a = \delta_p = \delta_m$), or (2) almost all available N is transported to larch ($f \cong 1$).

314 However, N immobilization by soil microorganisms (F_m) might not be a suitable

315 explanation, because it is generally accepted that immobilization is associated with

316 significant isotope fractionation, causing higher $\delta^{15}N$ in microorganisms than that of

317 substrate organic N [34,35]. Therefore, it is reasonable to consider that the observed

318 small $\Delta\delta^{15}N$ at boundary sites show that available N produced in the soil is mostly

319 transported to larch without significant fractionation. In contrast, large difference in

320 $\delta^{15}N$ between larch needle and soil ($\Delta\delta^{15}N < 0$) in forest sites (Figure 5(b)) suggests that

321 the ^{15}N-depleted part of available N is transported to larch, whereas the ^{15}N-enriched

322 part of available N is immobilized in soil microorganisms ($\delta_p < \delta_m$). This process is

323 consistent with previously observed ^{15}N enrichment in soil microorganisms during

324 immobilization [34,35], or with ^{15}N enrichment in the mycorrhizal fungal body and

325 ^{15}N-depletion in the host plant [36,37]. In fact, the observed magnitude of $\Delta\delta^{15}$N at

326 TR1n (8‰) was within the range of isotopic fractionation caused by ectomycorrhizal

327 fungi (5‰ to 9‰) [38], although such large enrichment is not always observed [26].

328 Interpretations of $\Delta\delta^{15}$N described above are also supported by other observed data. At

329 boundary sites, a high needle N concentration, a low C/N ratio of bulk soil, and a high

330 needle δ^{13}C were observed (Figure 5(a), 5(c), and 5(d)). Foliar N concentration and δ^{13}C

331 have been frequently used as indicators of N availability for trees [39] and light and

332 moisture conditions for plants [40], whereas the soil C/N as an indicator of the

333 decomposition rate of soil organic matter [41]. Therefore, these parameters as well as

334 the high NO_3^- to NH_4^+ ratios at boundary sites in MM area (Table S1) indicate a rapid

335 decomposition of soil organic matter and high N availability for larch under sunny and

336 dry conditions. On the other hand, at forest sites forest, a low needle N concentration, a

337 high C/N ratio of bulk soil, and a low needle δ^{13}C were observed (Figure 5(a), 5(c), and

338 5(d)), indicating the slow decomposition of soil organic matter and low N availability

339 for larch under shady and relatively wet conditions. Our results suggest that the

340 quantitative importance of the immobilization of available N, which is in agreement

341 with a previous study that showed the severe competition of available N between plant

342 and soil microorganisms in taiga forest ecosystem [42].

343   In the mass balance equation, we assumed that the available N pool was theoretically

344 at a steady state condition. Strictly speaking, it is not always true, however, the input

345 and loss or their imbalance might not affect our interpretations described above.

346 Generally, recycled N within the plant-soil system provides the primary source of N for

347 biological activities in most terrestrial ecosystems [43]. Although there is not enough

348 data to evaluate the N budget at our study sites, we assume that recycled N is the

349 dominant flux compared with the input and loss fluxes in the plant-soil system. In taiga,

350 the annual N demand of larch has been reported at 1,500 mg N m^{-2} yr^{-1} near at Tura in

351 central Siberia [44], and 850 to 3,100 mg N m^{-2} yr^{-1} at Yakutsk in northeastern Siberia

352 [42]. The estimated N loss as leaching (< 10mg N m^{-2} yr^{-1}) at Tura [44] and N input as

353 deposition (48 mg N m^{-2} yr^{-1}) at Yakutsk [42] were much smaller than the N demand.

354   In TR area, N deposition has been observed to be 96 to 289 mg N m^{-2} yr^{-1} [45], much

355 smaller than the forest N demand estimated in central and northeastern Siberia.

356 Furthermore it is unlike that N deposition causes spatial variation in $\delta^{15}N$ observed at

357 such small spatial scale (less than 2 km) in each area, because the amount and isotopic

358 composition of N deposition may be similar at all sites in each area. Although an uptake

359 of atmospheric deposited N by forest canopy has been reported to be a significant N

360   source for trees in the region where atmospheric pollution is severe [46], it may not

361   affect our results for similar reasons described above.

362   Leaching (F_{leach}) seems to be insignificant in the boundary, since no runoff has been

363   reported at the grassland in TR area; whereas it may occur on the north-facing slope in

364   the forest [47]. However, leaching leads to loss of ^{15}N-depleted N (such as NO_3^-), which

365   causes ^{15}N enrichment in available N especially inorganic N in the soil [48]. This

366   process is opposite to our interpretation to bear large $\Delta\delta^{15}$N in the forest (i.e. larch

367   uptake ^{15}N-depleted N which exists in the soil). The loss of N through N_2O gas emission

368   seems to be very small, as shown in the temperate steppe (17 to 28 mg N m^{-2} yr^{-1}) [49].

369   Therefore, both N input and loss processes may not be suitable to explain the variation

370   in $\Delta\delta^{15}$N observed in this study.

371   In the above mass balance, we assumed that only the 0-20 cm soil layer provided

372   available N to larch; however, the organic layer may also provide available N [50]. The

373   organic layer showed lower δ^{15}N than the bulk soil (Figure 3), suggesting that the δ^{15}N

374   of available N produced in the organic layer might be lower than that in the 0-20 cm soil

375   layer [51]. In the forest, where thick organic layer accumulates on the mineral soil layer,

376   larch uptake available N not only from the mineral soil layer, but also from the organic

377   layer; therefore, this additional uptake of lower δ^{15}N of available N from the organic

378   layer might contribute to large $\Delta\delta^{15}N$.

379   Recently, global syntheses of $\delta^{15}N$ values of plant and soil have been done by

380   comparing the $\delta^{15}N$ data with climate variables such as mean annual temperature (MAT)

381   and precipitation (MAP). Amundson et al. [14] compiled the $\delta^{15}N$ values from previous

382   studies, performed regression analysis, and successfully formulated plant and soil $\delta^{15}N$

383   and their difference ($\Delta\delta^{15}N$) with MAT and MAP. In addition, Craine et al. [15]

384   compiled foliar $\delta^{15}N$ and showed that foliar $\delta^{15}N$ increased with MAT at a rate of

385   0.23‰ $°C^{-1}$ for ecosystems with MAT > −0.5°C, and decreased by 2.6‰ for every order

386   of magnitude increase of MAP. Similarly, Craine et al. [16] conducted an analysis with

387   compiled soil $\delta^{15}N$, and reported that soil $\delta^{15}N$ increased with MAT at a rate of

388   0.18‰ $°C^{-1}$ for ecosystems with MAT > 9.8°C, showed no with MAT below 9.8°C, and

389   decreased at a rate of 1.78‰ for every order of magnitude increase of MAP. Plant $\delta^{15}N$

390   values calculated for the MAT and MAP of TR and MM areas with the multi regression

391   equation by Amundson et al. [14] derive -1.1‰ for TR area and -0.8‰ for MM area,

392   and those values are close to the average for all sites in this study (+1.5 (±2.2)‰).

393   Observed range in needle $\delta^{15}N$ (-3.9‰ to +4.3‰) also drops to the ranges of foliar $\delta^{15}N$

394   for both MAT and MAP as shown by Craine et al. [15]. Similarly, soil $\delta^{15}N$ values were

395   calculated to be +3.2‰ and +3.4‰ with MAT and MAP for both TR and MM areas by

396 the multi regression equation [14], and these values are also close to the average for all

397 sites in this study (+5.2 (±1.0)‰). The observed range of soil $\delta^{15}N$ (+2.9‰ to +7.4‰) is

398 also within the range reported by Craine et al. [16]. It is worth noting that a large

399 difference in $\delta^{15}N$ values was observed between forest and boundary sites, but average

400 $\delta^{15}N$ values observed for all sites, nevertheless, are close to the values obtained from

401 global syntheses.

402 As described above, global distributions of foliar and soil $\delta^{15}N$, and their difference

403 ($\Delta\delta^{15}N$) depend on climate parameters [14–16]. The global map of $\Delta\delta^{15}N$ reported by

404 Amundson et al. [14] is therefore corresponding to the vegetation that also depends on

405 the climate [1]. $\Delta\delta^{15}N$ is larger in boreal forest and smaller in temperate grassland as

406 seen in their global map, and this trend is exactly consistent with this study. Here we

407 propose that the accumulation of organic layer, as a comprehensive process of N cycling

408 in the ecosystem, can be regarded as a key process which controls $\Delta\delta^{15}N$.

409

410

411 **5.   Concluding remarks**

412 At a forest-grassland boundary in northern Mongolia, larch needle and soil $\delta^{15}N$ were

413 investigated to understand the mechanisms that control the spatial pattern of $\delta^{15}N$. The

414   difference between needle and soil $\delta^{15}N$ ($\Delta\delta^{15}N$) showed clear spatial variation along

415   the forest-grassland gradient with large $\Delta\delta^{15}N$ in the forest (up to -8‰) and small $\Delta\delta^{15}N$

416   in the grassland boundary (up to -2‰). The difference in $\delta^{15}N$ between larch and

417   mineral soil reflects the difference in the accumulation patterns of the organic layer. In

418   the grassland boundary, litter decomposes quickly and produced available N is

419   transported to larch without significant fractionation, whereas in the forest, larch trees

420   uptake available N with lower $\delta^{15}N$ than that produced in the soil. Namely, the

421   ^{15}N-depleted part is taken by larch, whereas the ^{15}N-enriched part remains in the soil,

422   which is balanced by ^{15}N-depleted litter provided by larch. The divergence of available

423   N between larch and microorganisms in the soil, and the accumulation of diverged N in

424   the organic layer control the variation in $\Delta\delta^{15}N$.

425

426

434

435

436   **References**

437   [1] Ågren GI, Andersson FO. Terrestrial ecosystem ecology: principles and applications.

438   Cambridge University Press; 2012.[2] Ometto J, Ehleringer JR, Domingues TF, Berry

439   JA, Ishida FY, Mazzi E, et al. The stable carbon and nitrogen isotopic composition of

440   vegetation in tropical forests of the Amazon Basin, Brazil. Biogeochemistry.

441   2006;79(1-2):251-74. doi: 10.1007/s10533-006-9008-8. PubMed PMID:

442   WOS:000240033100013.

443   [3] Hogbom L, Nilsson U, Orlander G. Nitrate dynamics after clear felling monitored

444   by in vivo nitrate reductase activity (NRA) and natural N-15 abundance of Deschampsia

445   flexuosa (L.) Trin. Forest Ecology and Management. 2002;160(1-3):273-80. doi:

446   10.1016/s0378-1127(01)00475-3. PubMed PMID: WOS:000175374500023.

447   [4] Houlton BZ, Sigman DM, Hedin LO. Isotopic evidence for large gaseous nitrogen

448   losses from tropical rainforests. Proceedings of the National Academy of Sciences of the

449   United States of America. 2006;103(23):8745-50. doi: 10.1073/pnas.0510185103.

450   PubMed PMID: WOS:000238278400031.

451   [5] Frank DA, Groffman PM, Evans RD, Tracy BF. Ungulate stimulation of nitrogen

452   cycling and retention in Yellowstone Park grasslands. Oecologia. 2000;123(1):116-21.

453   doi: 10.1007/s004420050996. PubMed PMID: WOS:000086884300014.

454   [6] Hobbie EA, Macko SA, Williams M. Correlations between foliar delta N-15 and

455   nitrogen concentrations may indicate plant-mycorrhizal interactions. Oecologia.

456   2000;122(2):273-83. doi: 10.1007/pl00008856. PubMed PMID:

457   WOS:000085386700015.

458   [7] Evans RD. Physiological mechanisms influencing plant nitrogen isotope

459   composition. Trends in Plant Science. 2001;6(3):121-6. doi:

460   10.1016/s1360-1385(01)01889-1. PubMed PMID: WOS:000167576600012.

461   [8] Zech M, Bimueller C, Hemp A, Samimi C, Broesike C, Hoerold C, et al. Human and

462   climate impact on N-15 natural abundance of plants and soils in high-mountain

463   ecosystems: a short review and two examples from the Eastern Pamirs and Mt.

464   Kilimanjaro. Isotopes in Environmental and Health Studies. 2011;47(3):286-96. doi:

465   10.1080/10256016.2011.596277. PubMed PMID: WOS:000299723800006.

466   [9] Nadelhoffer KJ, Fry B. Nitrogen isotope studies in forest ecosystems. In : Lajtha K,

467   Michener RH. Stable isotopes in ecology and environmental science. Blackwell

468   Scientific Publications; 1994. p. 22-44.

469   [10] Schulze ED, Chapin FS, Gebauer G. NITROGEN NUTRITION AND ISOTOPE

470   DIFFERENCES AMONG LIFE FORMS AT THE NORTHERN TREELINE OF

471   ALASKA. Oecologia. 1994;100(4):406-12. doi: 10.1007/bf00317862. PubMed PMID:

472   WOS:A1994QC13000008.

473   [11] Gebauer G, Giesemann A, Schulze ED, Jager HJ. ISOTOPE RATIOS AND

474   CONCENTRATIONS OF SULFUR AND NITROGEN IN NEEDLES AND SOILS OF

475   PICEA-ABIES STANDS AS INFLUENCED BY ATMOSPHERIC DEPOSITION OF

476   SULFUR AND NITROGEN-COMPOUNDS. Plant and Soil. 1994;164(2):267-81. doi:

477   10.1007/bf00010079. PubMed PMID: WOS:A1994PV72100013.

478   [12] Gebauer G, Schulze ED. CARBON AND NITROGEN ISOTOPE RATIOS IN

479   DIFFERENT COMPARTMENTS OF A HEALTHY AND A DECLINING

480   PICEA-ABIES FOREST IN THE FICHTELGEBIRGE, NE BAVARIA. Oecologia.

481   1991;87(2):198-207. doi: 10.1007/bf00325257. PubMed PMID:

482   WOS:A1991FX12200006.

483   [13] Jung K, Gebauer G, Gehre M, Hofmann D, Weissflog L, Schuurmann G.

484   Anthropogenic impacts on natural nitrogen isotope variations in Pinus sylvestris stands

485   in an industrially polluted area. Environmental Pollution. 1997;97(1-2):175-81. doi:

486   10.1016/s0269-7491(97)00053-5. PubMed PMID: WOS:A1997YD75800021.

487   [14] Amundson R, Austin AT, Schuur EAG, Yoo K, Matzek V, Kendall C, et al. Global

488   patterns of the isotopic composition of soil and plant nitrogen. Global Biogeochemical

489   Cycles. 2003;17(1). doi: 10.1029/2002gb001903. PubMed PMID:

490   WOS:000182817800001.

491   [15] Craine JM, Elmore AJ, Aidar MPM, Bustamante M, Dawson TE, Hobbie EA, et al.

492   Global patterns of foliar nitrogen isotopes and their relationships with climate,

493   mycorrhizal fungi, foliar nutrient concentrations, and nitrogen availability. New

494   Phytologist. 2009;183(4):980-92. doi: 10.1111/j.1469-8137.2009.02917.x. PubMed

495   PMID: WOS:000268855300008.

496   [16] Craine JM, Elmore AJ, Wang LX, Augusto L, Baisden WT, Brookshire ENJ, et al.

497   Convergence of soil nitrogen isotopes across global climate gradients. Scientific

498   Reports. 2015;5. doi: 10.1038/srep08280. PubMed PMID: WOS:000348903800001.

499   [17] Pardo LH, Hemond HF, Montoya JP, Pett-Ridge J. Natural abundance N-15 in soil

500   and litter across a nitrate-output gradient in New Hampshire. Forest Ecology and

501   Management. 2007;251(3):217-30. doi: 10.1016/j.foreco.2007.06.047. PubMed PMID:

502   WOS:000250743000009.

503   [18] Garten CT, Vanmiegroet H. RELATIONSHIPS BETWEEN SOIL-NITROGEN

504   DYNAMICS AND NATURAL N-15 ABUNDANCE IN PLANT FOLIAGE FROM

505   GREAT SMOKY MOUNTAINS NATIONAL-PARK. Canadian Journal of Forest

506   Research-Revue Canadienne De Recherche Forestiere. 1994;24(8):1636-45. doi:

507   10.1139/x94-212. PubMed PMID: WOS:A1994QA52700014.

508   [19] Brenner DL, Amundson R, Baisden WT, Kendall C, Harden J. Soil N and N-15

509   variation with time in a California annual grassland ecosystem. Geochimica Et

510   Cosmochimica Acta. 2001;65(22):4171-86. doi: 10.1016/s0016-7037(01)00699-8.

511   PubMed PMID: WOS:000172349700007.

512   [20] Averill C, Finzi AC. Increasing plant use of organic nitrogen with elevation is

513   reflected in nitrogen uptake rates and ecosystem delta N-15. Ecology.

514   2011;92(4):883-91. doi: 10.1890/10-0746.1. PubMed PMID: WOS:000290533700010.

515   [21] Callesen I, Nilsson LO, Schmidt IK, Vesterdal L, Ambus P, Christiansen JR, et al.

516   The natural abundance of N-15 in litter and soil profiles under six temperate tree

517   species: N cycling depends on tree species traits and site fertility. Plant and Soil.

518   2013;368(1-2):375-92. doi: 10.1007/s11104-012-1515-x. PubMed PMID:

519   WOS:000321641700028.

520   [22] Brearley FQ. Nitrogen stable isotopes indicate differences in nitrogen cycling

521   between two contrasting Jamaican montane forests. Plant and Soil.

522   2013;367(1-2):465-76. doi: 10.1007/s11104-012-1469-z. PubMed PMID:

523   WOS:000319771700033.

524   [23] Emmett BA, Kjonaas OJ, Gundersen P, Koopmans C, Tietema A, Sleep D. Natural

525   abundance of N-15 in forests across a nitrogen deposition gradient. Forest Ecology and

526   Management. 1998;101(1-3):9-18. doi: 10.1016/s0378-1127(97)00121-7. PubMed

527   PMID: WOS:000072095800002.

528   [24] Schuur EAG, Matson PA. Net primary productivity and nutrient cycling across a

529   mesic to wet precipitation gradient in Hawaiian montane forest. Oecologia.

530   2001;128(3):431-42. doi: 10.1007/s004420100671. PubMed PMID:

531   WOS:000170499400015.

532   [25] Hobbie EA, Macko SA, Shugart HH. Insights into nitrogen and carbon dynamics

533   of ectomycorrhizal and saprotrophic fungi from isotopic evidence. Oecologia.

534   1999;118(3):353-60. doi: 10.1007/s004420050736. PubMed PMID:

535   WOS:000079391900009.

536   [26] Gebauer G, Meyer M. N-15 and C-13 natural abundance of autotrophic and

537   mycoheterotrophic orchids provides insight into nitrogen and carbon gain from fungal

538   association. New Phytologist. 2003;160(1):209-23. doi:

539   10.1046/j.1469-8137.2003.00872.x. PubMed PMID: WOS:000185557300024.

540 [27] Garten CT. VARIATION IN FOLIAR N-15 ABUNDANCE AND THE

541 AVAILABILITY OF SOIL-NITROGEN ON WALKER BRANCH WATERSHED.

542 Ecology. 1993;74(7):2098-113. doi: 10.2307/1940855. PubMed PMID:

543 WOS:A1993LY54900021.

544 [28] Li SG, Asanuma J, Kotani A, Eugster W, Davaa G, Oyunbaatar D, Sugita M.

545 Year-round measurements of net ecosystem CO_2 flux over a montane larch forest in

546 Mongolia. Journal of Geophysical Research-Atmospheres 110. 2005. doi:

547 10.1029/2004jd005453

548 [29] Ishikawa M, Sharkuu N, Zhang YS, Kadota T, Ohata TT. Ground thermal and

549 moisture conditions at the southern boundary of discontinuous permafrost, Mongolia.

550 Permafrost and Periglacial Processes. 2005;16(2):209-16. doi: 10.1002/ppp.483.

551 PubMed PMID: WOS:000229979600006.

552 [30] Peel MC, Finlayson BL, McMahon TA. Updated world map of the Koppen-Geiger

553 climate classification. Hydrology and Earth System Sciences. 2007;11(5):1633-44.

554 PubMed PMID: WOS:000251516100009.

555 [31] Tuhkanen S. Treeline in relation to climate, with special reference to oceanic areas.

556 In : Alden JN, Mastrantonio JL, Ødum S. Forest development in cold climates. Springer

557 US; 1993. p. 115-134.

558   [32] Ponge JF. Humus forms in terrestrial ecosystems: a framework to biodiversity. Soil

559   Biology & Biochemistry. 2003;35(7):935-45. doi: 10.1016/s0038-0717(03)00149-4.

560   PubMed PMID: WOS:000184125500007.

561   [33] Hobbie EA, Ouimette AP. Controls of nitrogen isotope patterns in soil profiles.

562   Biogeochemistry. 2009;95(2-3):355-71. doi: 10.1007/s10533-009-9328-6. PubMed

563   PMID: WOS:000269837900012.

564   [34] Dijkstra P, LaViolette CM, Coyle JS, Doucett RR, Schwartz E, Hart SC, et al. N-15

565   enrichment as an integrator of the effects of C and N on microbial metabolism and

566   ecosystem function. Ecology Letters. 2008;11(4):389-97. doi:

567   10.1111/j.1461-0248.2008.01154.x. PubMed PMID: WOS:000254628000010.

568   [35] Coyle JS, Dijkstra P, Doucett RR, Schwartz E, Hart SC, Hungate BA.

569   Relationships between C and N availability, substrate age, and natural abundance C-13

570   and N-15 signatures of soil microbial biomass in a semiarid climate. Soil Biology &

571   Biochemistry. 2009;41(8):1605-11. doi: 10.1016/j.soilbio.2009.04.022. PubMed PMID:

572   WOS:000268920400003.

573   [36] Gebauer G, Dietrich P. Nitrogen isotope ratios in different compartments of a

574   mixed stand of spruce, larch and beech trees and of understory vegetation including

575   fungi. Isotopes in Environmental and Health Studies. 1993;29(1-2):35-44. doi:

576   10.1080/10256019308046133.

577   [37] Michelsen A, Quarmby C, Sleep D, Jonasson S. Vascular plant N-15 natural

578   abundance in heath and forest tundra ecosystems is closely correlated with presence and

579   type of mycorrhizal fungi in roots. Oecologia. 1998;115(3):406-18. doi:

580   10.1007/s004420050535. PubMed PMID: WOS:000074877400017.

581   [38] Hobbie EA, Hogberg P. Nitrogen isotopes link mycorrhizal fungi and plants to

582   nitrogen dynamics. New Phytologist. 2012;196(2):367-82. doi:

583   10.1111/j.1469-8137.2012.04300.x. PubMed PMID: WOS:000308882200009. [39]

584   Liang MC, Sugimoto A, Tei S, Bragin IV, Takano S, Morozumi T, et al. Importance of

585   soil moisture and N availability to larch growth and distribution in the Arctic

586   taiga-tundra boundary ecosystem, northeastern Siberia. Polar Science. 2014;8(4):327-41.

587   doi: 10.1016/j.polar.2014.07.008. PubMed PMID: WOS:000346894800002.

588   [40] Farquhar GD, Ehleringer JR, Hubick KT. CARBON ISOTOPE

589   DISCRIMINATION AND PHOTOSYNTHESIS. Annual Review of Plant Physiology

590   and Plant Molecular Biology. 1989;40:503-37. doi: 10.1146/annurev.arplant.40.1.503.

591   PubMed PMID: WOS:A1989U857900019.

592   [41] Finzi AC, Van Breemen N, Canham CD. Canopy tree soil interactions within

593   temperate forests: Species effects on soil carbon and nitrogen. Ecological Applications.

594   1998;8(2):440-6. doi: 10.2307/2641083. PubMed PMID: WOS:000073447900023.

595   [42] Popova AS, Tokuchi N, Ohte N, Ueda MU, Osaka K, Maximov TC, et al. Nitrogen

596   availability in the taiga forest ecosystem of northeastern Siberia. Soil Science and Plant

597   Nutrition. 2013;59(3):427-41. doi: 10.1080/00380768.2013.772495. PubMed PMID:

598   WOS:000322809800014.

599   [43] Parton W, Silver WL, Burke IC, Grassens L, Harmon ME, Currie WS, et al.

600   Global-scale similarities in nitrogen release patterns during long-term decomposition.

601   Science. 2007;315(5810):361-4. doi: 10.1126/science.1134853. PubMed PMID:

602   WOS:000243535400037.

603   [44] Tokuchi N, Hirobe M, Kondo K, Arai H, Hobara S, Fukushima K, Matsuura Y.

604   Permafrost Ecosystems: Siberian Larch Forests. Springer: Netherlands; 2010. Soil

605   nitrogen dynamics in larch ecosystem; p. 229–243.

606   [45] EANET Data on the Acid Deposition in the East Asian Region (2002-2011)

607   [Internet]. Network Center for EANET. Available from:

608   http://www.eanet.asia/index.html

609   [46] Harrison AF, Schulze ED, Gebauer G, et al. Canopy uptake and utilization of

610   atmospheric pollutant nitrogen. In : Schulze ED. Carbon and nitrogen cycling in

611   European forest ecosystems. Springer-Verlag Berlin Heidelberg; 2000. p. 171-188.

612   [47] Iijima Y, Ishikawa M, Jambaljav Y. Hydrological cycle in relation to permafrost

613   environment in forest-grassland ecotone in Mongolia. Journal of Japanese Association

614   of Hydrological Sciences. 2012;42:119-130.

615   [48] Martinelli LA, Piccolo MC, Townsend AR, Vitousek PM, Cuevas E, McDowell W,

616   et al. Nitrogen stable isotopic composition of leaves and soil: Tropical versus temperate

617   forests. Biogeochemistry. 1999;46(1-3):45-65. doi: 10.1023/a:1006100128782. PubMed

618   PMID: WOS:000080776300004.

619   [49] Wolf B, Zheng XH, Brueggemann N, Chen WW, Dannenmann M, Han XG, et al.

620   Grazing-induced reduction of natural nitrous oxide release from continental steppe.

621   Nature. 2010;464(7290):881-4. doi: 10.1038/nature08931. PubMed PMID:

622   WOS:000276397300035.

623   [50] Tietema A, Warmerdam B, Lenting E, Riemer L. ABIOTIC FACTORS

624   REGULATING NITROGEN TRANSFORMATIONS IN THE ORGANIC LAYER OF

625   ACID FOREST SOILS - MOISTURE AND PH. Plant and Soil. 1992;147(1):69-78.

626   doi: 10.1007/bf00009372. PubMed PMID: WOS:A1992KK11100008.

627   [51] Koba K, Hirobe M, Koyama L, Kohzu A, Tokuchi N, Nadelhoffer KJ, et al. Natural

628   N-15 abundance of plants and soil N in a temperate coniferous forest. Ecosystems.

629   2003;6(5):457-69. doi: 10.1007/s10021-002-0132-6. PubMed PMID:

630   WOS:000185256000005.

631

632

633

634

635

636

637

638

639

640

641

642

643

644

645

646   Table 1. Locations of sampling sites.

Area name	code	Site No.[a] position	Latitude °N	Longitude °E	Elevation m
Terelj	TR	1n, 2n, 3n, 4n, 5n, 6n, 7n, 8n	47.97	107.42	1587-1750
		ic	47.98	107.40	1639
		1s, 2s	47.99	107.42	1651-1791
Mongonmorit	MM	1s, 2s, 3s, 4s, 5s, 6s, 7s	48.35	108.66	1525-1619
		1sw, 2sw, 3sw	48.35	108.65	1593-1623

647

648   [a] Each sampling site is expressed by area code and position on a slope. The position

649   number increases along upper to lower slope. The letter after position number indicates

650   the direction of slope. For example, "n" means north-facing slope and "sw" means

651   southwest-facing slope. TRic is a site in valley.

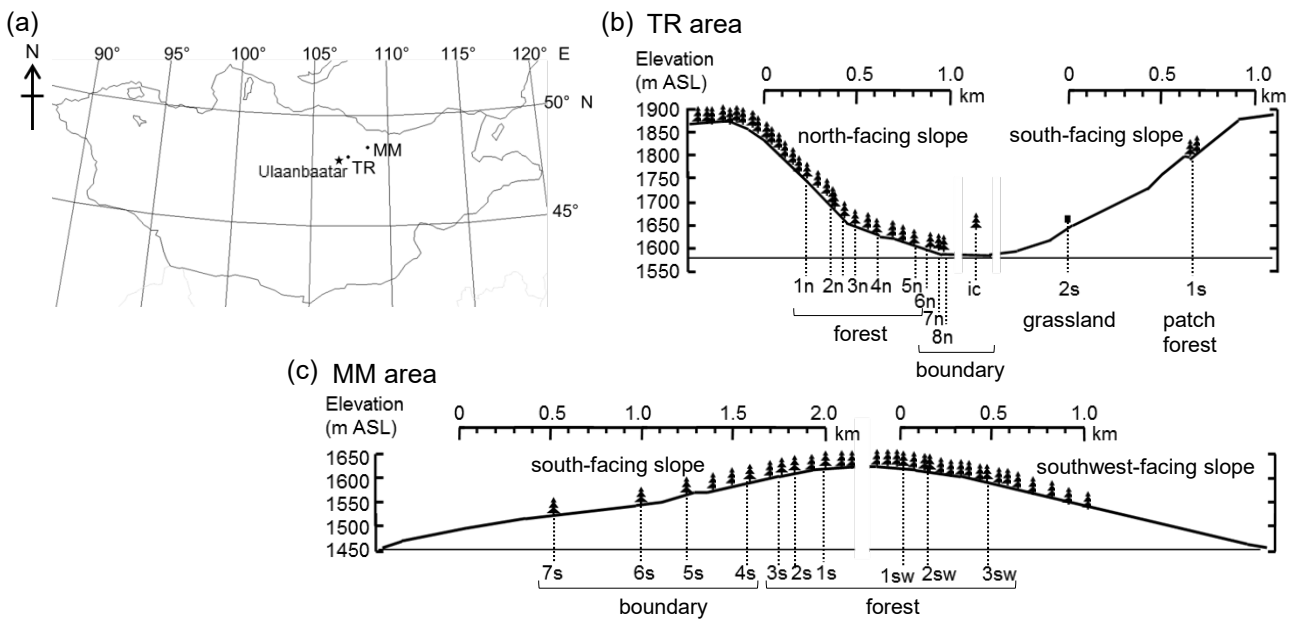652

653

654

655

656

657

658

659

660   Figure 1. A map of the two observation areas (TR and MM) and Ulaanbaatar, the capital

661   of Mongolia (a), and schematic figures of longitudinal cross sections in TR area (b) and

662   MM area (c). Samplings were conducted at Terelj (TR) and Mongonmorit (MM) at the

663   forest-grassland boundary in northern Mongolia. In TR area, sampling was conducted at

664   11 sites along a transect line from the north-facing slope to the south-facing slope over a

665   valley. In MM area, two transects were set on the south-facing slope and the

666   southwest-facing slope, and sampling was conducted at 10 sites.

667

668   Figure 2. Temporal variations in larch needle N concentration (a), $\delta^{15}N$ (b), and $\delta^{13}C$ (c)

669   in TR area. Data from two trees at TR3n, four trees at TR6n, and three trees at TR1s are

670   shown. Each tree is expressed by a different shape (circle, rectangle, or triangle) and

671   colour (black or white). Trees within the same site share the same shape.

672

673   Figure 3. Vertical profiles of larch needle, organic layer, and bulk soil $\delta^{15}N$ values at the

674   forest site (TR1n) and the boundary site (TR7n) in TR area. Bars represent standard

675   deviation of the mean.

676

677   Figure 4. Spatial variations in larch needle (triangle) and soil (square) $\delta^{15}N$ (a),

678   differences in $\delta^{15}N$ between needle and soil ($\Delta\delta^{15}N$) (b), and needle $\delta^{13}C$ (open-triangle)

679   and N concentration (filled-triangle) (c) in TR area, and the same as (d), (e), and (f) in

680   MM area. Bars represent standard deviation of the mean.

681

682   Figure 5. Correlations between larch needle $\delta^{13}C$ and $\delta^{15}N$ ($r_s = 0.877$) (a), needle and

683   soil $\delta^{15}N$ ($r_s = 0.718$) (b), needle N concentration and $\Delta\delta^{15}N$ ($r_s = 0.591$) (c), and C/N

684   ratio of bulk soil and $\Delta\delta^{15}N$ ($r_s = -0.541$) (d) at all sites in TR area (circle) and MM area

685   (triangle). Dotted lines in (b) indicate $\Delta\delta^{15}N$ values at 0‰, -4‰ and -8‰. Correlation

686   coefficients are significant at $p < 0.05$. Bars represent standard deviation of the mean.

Figure 1.

A map of the two observation areas (TR and MM) and Ulaanbaatar, the capital of Mongolia (a), and schematic figures of longitudinal cross sections in TR area (b) and MM area (c). Samplings were conducted at Terelj (TR) and Mongonmorit (MM) at the forest-grassland boundary in northern Mongolia. In TR area, sampling was conducted at 11 sites along a transect line from the north-facing slope to the south-facing slope over a valley. In MM area, two transects were set on the south-facing slope and the southwest-facing slope, and sampling was conducted at 10 sites.
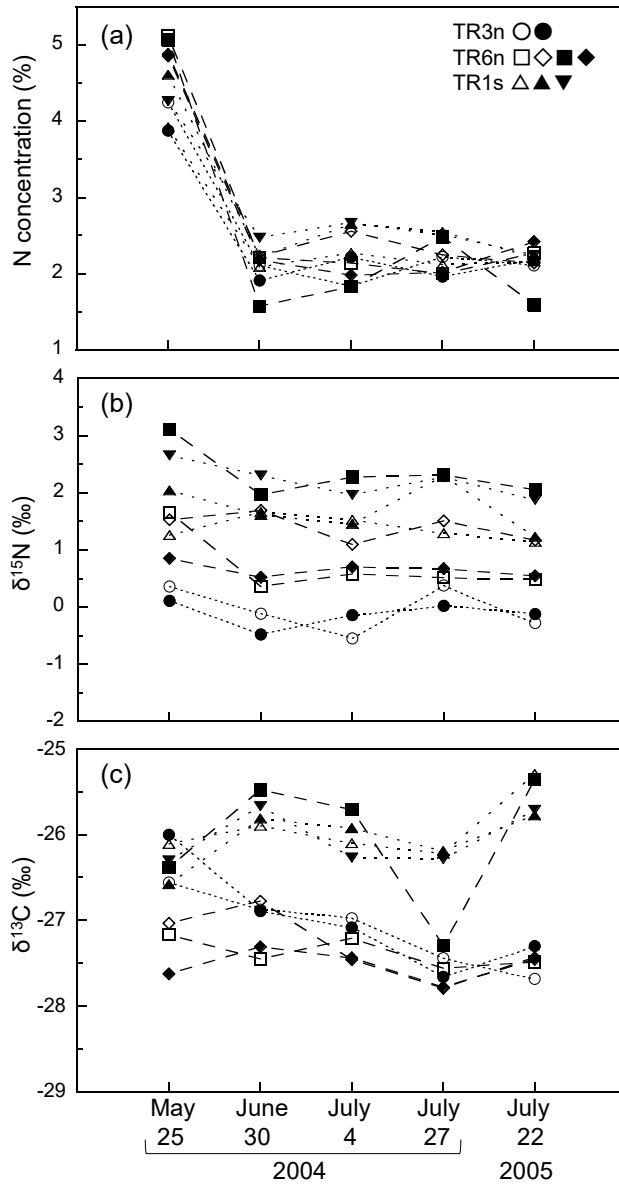
Figure 2.

Temporal variations in larch needle N concentration (a), $\delta^{15}N$ (b), and $\delta^{13}C$ (c) in TR area. Data

from two trees at TR3n, four trees at TR6n, and three trees at TR1s are shown. Each tree is

expressed by a different shape (circle, rectangle, or triangle) and colour (black or white). Trees
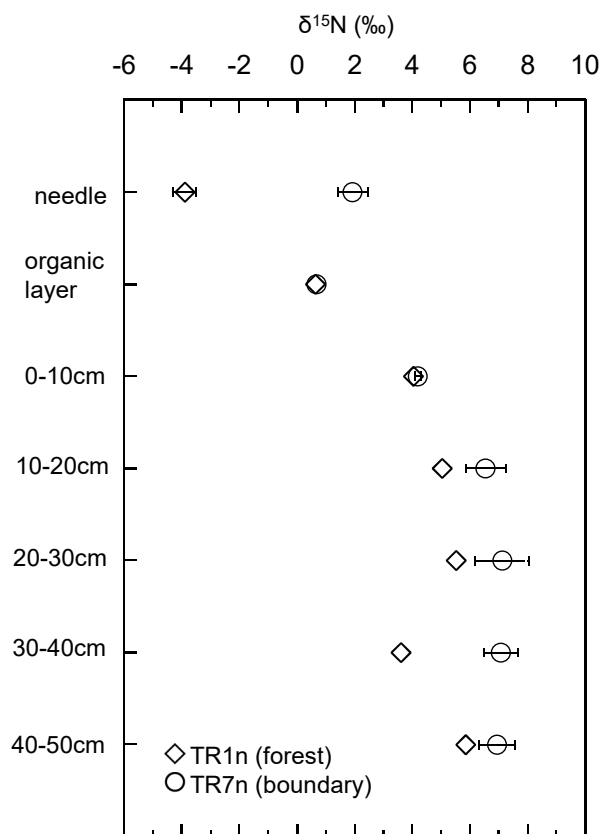
within the same site share the same shape.

Figure 3.

Vertical profiles of larch needle, organic layer, and bulk soil $\delta^{15}N$ values at the forest site (TR1n) and the boundary site (TR7n) in TR area. Bars represent standard deviation of the mean.
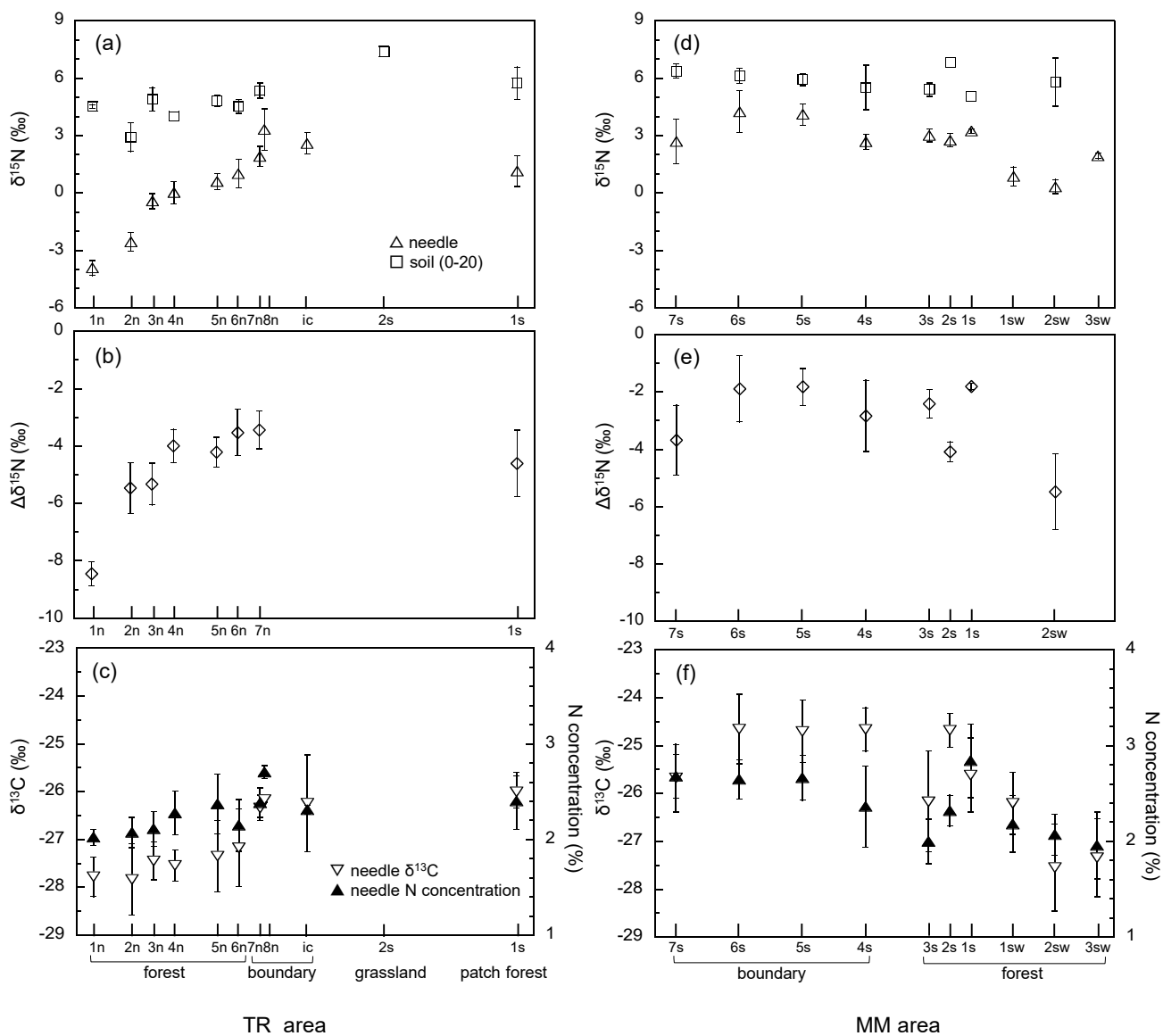
Figure 4.

Spatial variations in larch needle (triangle) and soil (square) $\delta^{15}N$ (a), differences in $\delta^{15}N$ between needle and

soil ($\Delta\delta^{15}N$) (b), and needle $\delta^{13}C$ (open-triangle) and N concentration (filled-triangle) (c) in TR area, and the

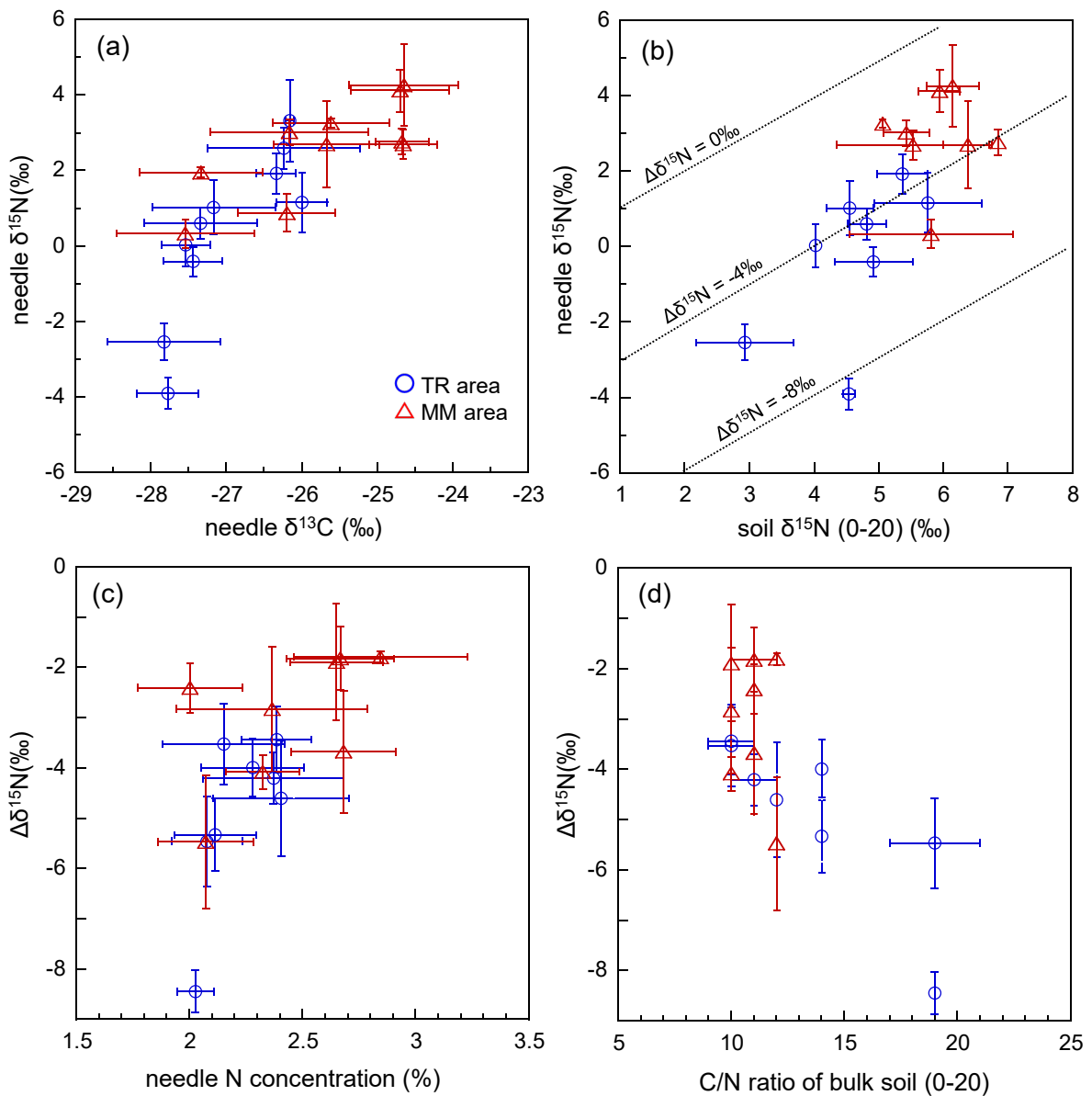same as (d), (e), and (f) in MM area. Bars represent standard deviation of the mean.

Figure 5.

Correlations between larch needle $\delta^{13}C$ and $\delta^{15}N$ ($r_s = 0.877$) (a), needle and soil $\delta^{15}N$ ($r_s = 0.718$) (b), needle N concentration and $\Delta\delta^{15}N$ ($r_s = 0.591$) (c), and C/N ratio of bulk soil and $\Delta\delta^{15}N$ ($r_s = -0.541$) (d) at all sites in TR area (circle) and MM area (triangle). Dotted lines in (b) indicate $\Delta\delta^{15}N$ values at 0‰, -4‰ and -8‰. Correlation coefficients are significant at $p < 0.05$. Bars represent standard deviation of the mean.
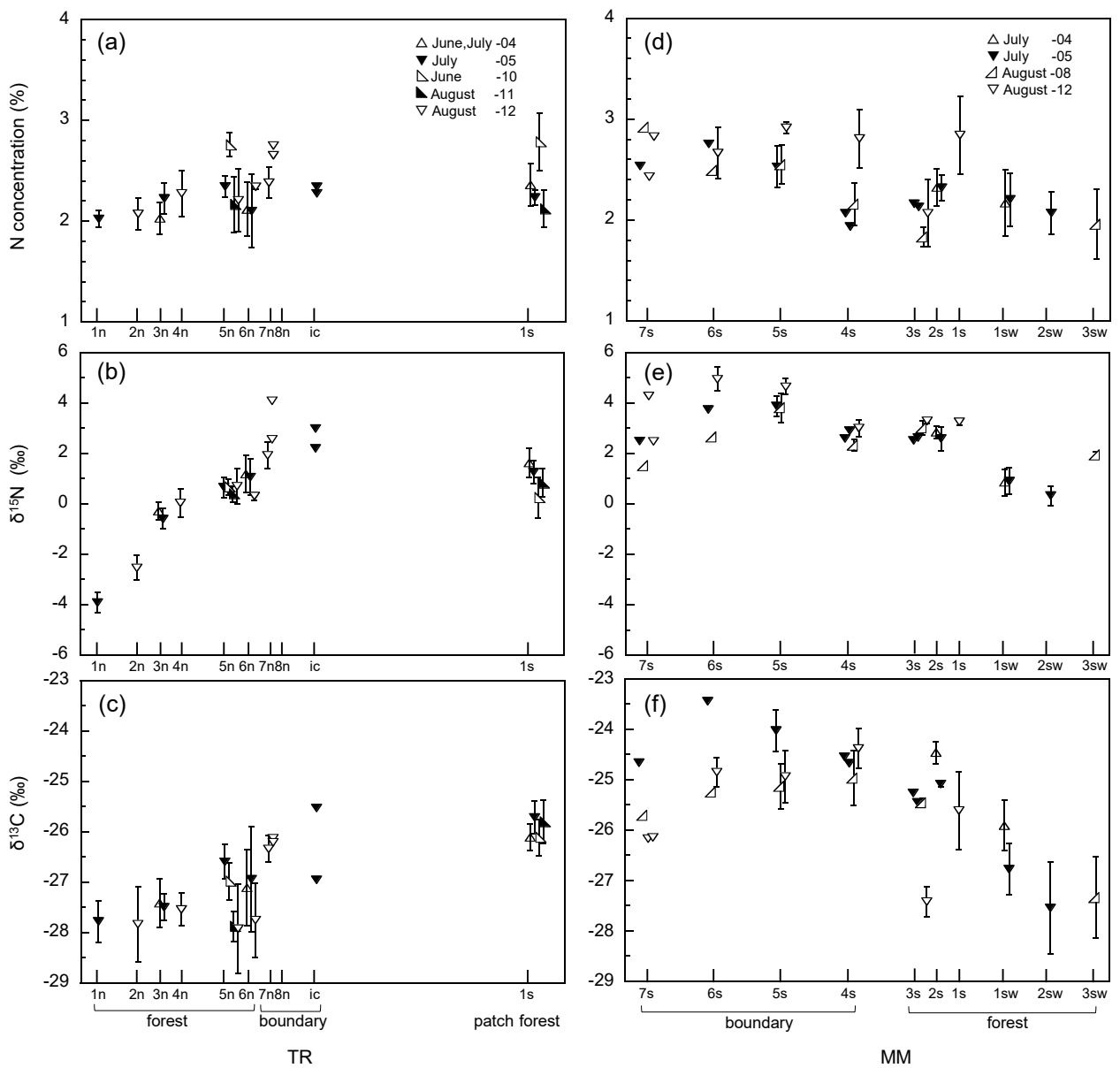
Figure S1.
Larch needle N concentration (a), $\delta^{15}N$ (b), and $\delta^{13}C$ (c) in TR area, and the same as (d), (e), and (f) in MM area observed on all sampling dates at each site . Bars represent standard deviation of the mean.
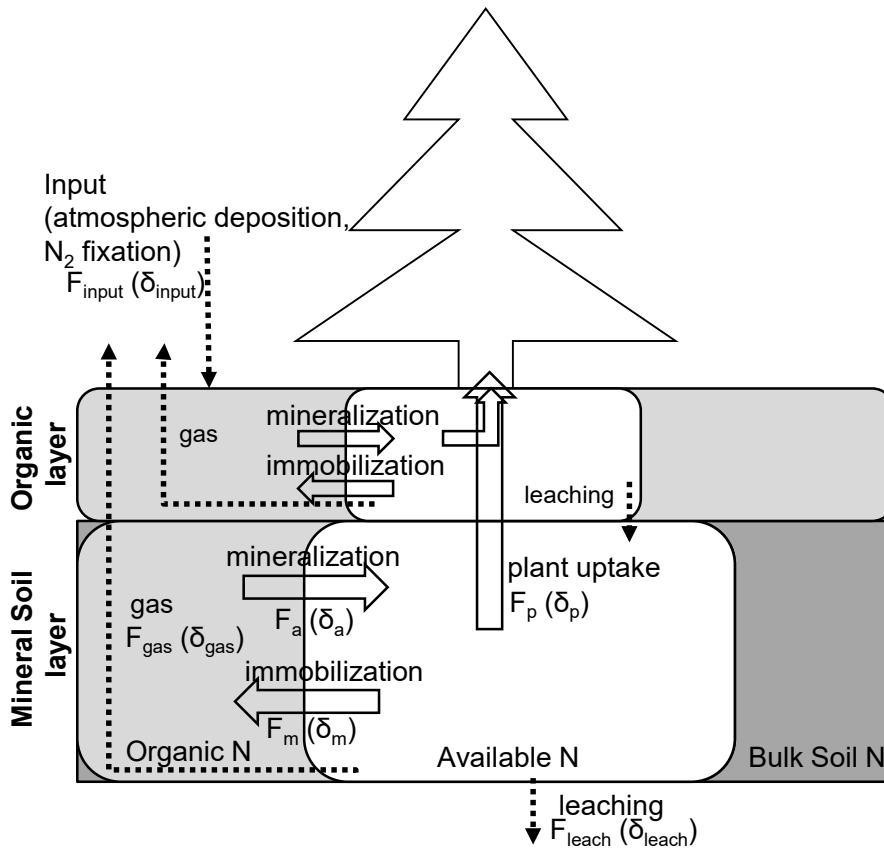
Figure S2.
The schematic representation of mass balance of biologically available N in plant-soil system.
Assuming that the available N pool is at a steady state, the following equations are established:

$$F_{input} + F_a = F_p + F_m + F_{leach} + F_{gas} \qquad (1)$$

and for $\delta^{15}N$,

$$F_{input} \times \delta_{input} + F_a \times \delta_a = F_p \times \delta_p + F_m \times \delta_m + F_{leach} \times \delta_{leach} + F_{gas} \times \delta_{gas} \qquad (2)$$

where F_{input} is the N derived from atmospheric N deposition and biological N_2 fixation, and F_a is the N produced in the soil through the decomposition of soil organic matter. F_p and F_m are the fluxes of available N taken up by plants and immobilized by soil microorganisms, respectively. F_{leach} and F_{gas} are the N lost due to leaching and gaseous emission, respectively. The values of δ_{input}, δ_a, δ_p, δ_m, δ_{leach}, and δ_{gas} are the $\delta^{15}N$ of input, produced N from soil organic matter, plant uptake, immobilization by soil microorganisms, leaching, and gaseous emission of available N, respectively. We assumed that larch was the only plant species (i.e. δ_p = needle $\delta^{15}N$), and that the $\delta^{15}N$ of available N produced in the soil was the same as that of the soil (i.e. δ_a = soil $\delta^{15}N$).